Pure Appl. Geophys. 171 (2014), 2537–2553

DOI 10.1007/s00024-013-0743-1

Pure and Applied Geophysics

Linking the Recurrence Time of Earthquakes to Source Parameters: A Dream or a Real Possibility?

Andrea Bizzarri[1] and Paola Crupi[2]

Abstract—By using a single-degree-of-freedom spring-slider analog fault model, we generate a synthetic catalog of nearly 500 different seismic sequences. We explore the parameter space by assuming different values of constitutive parameters and tectonic environment. We also consider three different versions of the rate-dependent and state-dependent friction laws [the Dieterich-Ruina (DR), the Ruina-Dieterich (RD) and the Chester-Higgs (CH) models], and different approximations of the behavior of the friction at high sliding speeds, as well as the radiation damping effects. Our results indicate that for all the considered models, the recurrence time (T_{cycle}) exhibits an inverse proportionality on the loading rate; a linear, positive dependence on the effective normal stress; and a linear, negative dependence on the characteristic distance controlling the state variable evolution. These results confirm and generalize previous studies. Remarkably, we found here that the coefficients of proportionality strongly depend on the adopted friction model, on the high speed behavior and on the reference set of parameters. Notably, we also found that the positive proportionality between T_{cycle} and the difference $b - a$, confirmed for DR and RD laws, does not hold in general for the CH law. Overall, we conclude that even in the simplest (and idealized) case of characteristic earthquakes considered here, in which the limiting cycle is reached by the system, and even in the framework of a very simplified fault model, the possibility to a priori predict, through an universal analytical relation, the inter-event time of an impending earthquake still remains only a dream. On the other hand, a numerical prediction of T_{cycle} would require the exact knowledge of the rheological model (and its parameters at all times over the entire life of the fault) and the actual state of the fault, which indeed are often unknown.

Key words: Fault mechanics, recurrence time, earthquake prediction, constitutive models, computational seismology.

1. Introduction

The grand challenge of seismology is to predict earthquakes, which is not only a very important scientific goal, but is also a major societal objective, both in terms of human losses and economic damages.

Contrary to other ambits of physics (e.g., in quantum mechanics the Heisenberg's uncertainty principle establishes that it is theoretically impossible to exactly predict the position and the momentum of a particle, simultaneously; Heisenberg 1927), there are no theoretical reasons impeding the spatio–temporal prediction of an earthquake event (Bizzarri 2012b). Despite technical and epistemic difficulties, the prediction of earthquakes still remains a prominent objective for the entire scientific community. Indeed, seismology is a relatively young discipline, and it suffers some severe limitations, represented by (1) the epistemic, relatively incomplete understanding of the physics of earthquakes; and by (2) the ignorance about the state of stress of the faults. In other words, our knowledge of both the equations to be solved (more explicitly, the fault constitutive model, which complements the equation of motion) and of the initial conditions is still lacking, making the physics of the earthquake source a very peculiar exact science. Moreover, we do not have the possibility to plan experiments at the real-world scale, such as scientists in the fields of high energy physics or molecular biology do. On the other hand, we can perform cutting-edge numerical simulations, but do not yet have yet a general consensus on the most appropriate equations to describe the physical behavior of a seismic source (see Bizzarri 2011b for a thorough review). This is in contrast, for instance,

[1] Istituto Nazionale di Geofisica e Vulcanologia, Sezione di Bologna, Via Donato Creti, 12, 40128 Bologna, Italy. E-mail: bizzarri@bo.ingv.it

[2] Dipartimento di Scienze della Terra e Geoambientali, Università degli Studi di Bari, Via Orabona 4, 70125 Bari, Italy. E-mail: paola.crupi@uniba.it

to climatology, which still can not plan experiments, but knows the equations describing the problems to be handled.

Statistical analysis—which accepts that several properties of the faulting processes are out of range and can be described only in probability terms (Vere-Jones 2010)—relies on seismological records, and is therefore affected by the relative infrequency of large events. These events can then provide only a limited data set for the study of their impact on modern cities (e.g., Allen 2007). Moreover, some authors have shown (Wyss *et al.* 2012; Kossobokov and Nekrasova 2012; see also Zuccolo *et al.* 2011) that the seismic hazard maps generated by the Global Seismic Hazard Assessment Program (GSHAP; www.seismo.ethz.ch/static/GSHAP), do not correctly give the seismic hazard for disastrous earthquakes with $M \in (6.9, 8.6)$. Indeed, Kossobokov and Nekrasova (2012), by performing a quantitative comparison between the GSHAP maps and the factual effects under strong earthquakes, formulate a verdict useless for this kind of probabilistic product in the framework of any type of seismic hazard evaluation. The scientific debate on this topic is indeed vigorous (see for instance Panza *et al.* 2011, 2012). It is also true that during the last 50 years there have been insufficient seismological records to constrain the dynamics of a seismogenic fault over a time window of 100–1,000 years. In other words, the earthquake cycle could often be far larger than the duration of the instrumental, scientific observations.

The physical (or deterministic) description of earthquake sources—which excludes any random process—is affected by the epistemic, severe limitations discussed above. Finally, we mention here that the so-called neo-deterministic seismic hazard analysis (NDSHA)—which originated after a careful scrutiny of the standard hazard maps (Wyss *et al.* 2012)—produces a set synthetic ground motions based upon the physics of the earthquake source and wave propagation models (e.g., Panza *et al.* 2001; Zuccolo *et al.* 2011 and referenced cited therein).

By considering a single-degree-of-freedom mass-spring analog fault model (e.g., Gu *et al.* 1984), Bizzarri (2012b) emphasizes that a large number of factors can dramatically influence the recurrence time T_{cycle}; (1) fault interactions and stress triggering phenomena, (2) the analytical expression of the fault governing law, (3) the thermally-activated pressurization of pore fluids, (4) wear processes, (5) the variations of the hydraulic properties of the fault zone (such as permeability and porosity) and (6) the Arrhenius nature of the so-called direct effect in the framework of the rate-dependent and state-dependent friction laws (e.g., Ruina 1983). Moreover, (7) Crupi and Bizzarri (2013) demonstrate that the analytical formulation of the equation of motion of the spring–slider system (more explicitly, the incorporation of the contribution of the energy lost as radiating waves, ignored for a long time in previous 1-D models) has relevant consequences in the determination of the seismic cycle time. Finally, (8) Bizzarri and Crupi (2013) point out that even the initial thermal state of the fault can have significant effect on the prediction of T_{cycle} in the framework of a rate-dependent, state-dependent and temperature-dependent fault rheology (Chester and Higgs 1992). All these results can somehow endanger the concept itself of seismic cycle.

In this paper, we intentionally neglect all the above-mentioned complications, and assume a constant effective normal stress. We consider a perfectly homogeneous and isolated fault, so that the 1-D spring-slider model adopted in the numerical computation presented and discussed in the present study can be adequate to describe, at least as a first-order approximation, such a seismogenic system; the limitations of the model are discussed in more details in Sect. 4. By conducting a large number of numerical experiments (we produce an ensemble of nearly 500 different seismic sequences), we analyze whether it is possible to extract from our catalog of synthetic events a universal, analytical (empirical) equation that can fit all the data, with the aim to explore whether it is possible to analytically express a priori the cycle time as a function of the source parameters.

2. Methodology

As anticipated in the previous section, we consider the single-degree-of-freedom spring-slider model, so that the we deal with a 1-D fault model, in which the unique independent variable is time.

The analytical and numerical details are summarized in Appendix A. The fault system can be governed by different formulations of the rate-dependent and state-dependent friction laws, namely the Dieterich-Ruina (Dieterich 1994), the Ruina-Dieterich (Ruina 1983) and the Chester-Higgs (Chester and Higgs 1992) constitutive models (for the remainder of the present paper, we will refer to those laws with the notations DR, RD and CH, respectively). In these fault governing models, recalled for completeness in Appendix A [see Eqs. (8), (9) and (10)], there are basically three constitutive parameters; a, which accounts for the so-called direct effect and represents a velocity-hardening preparatory stage in the early stages of the rupture; b, which controls the evolutionary effects and basically describes the stress release process; and L, which represents the characteristic slip distance over which the state variable Ψ evolves. The latter physically accounts for the memory effects (i.e., previous slip instability episodes) of the sliding interface, and has a different meaning (and dimension), depending on the adopted model (see Bizzarri 2011b; his Sect. 7).

We consider two rather different configurations, listed in Table 1. Configuration A, which is configuration A of Crupi and Bizzarri (2013), corresponds to a strong velocity-weakening regime, characterizing a fault with a relatively high degree of instability. Configuration B, taken from Lapusta and Barbot (2012) and Barbot *et al.* (2012), still defines a velocity-weakening regime, but with a lower degree of instability. We also emphasize that, changing from configuration A to configuration B, we do not only modify the constitutive parameters a and b, but also the hypocentral depth (and thus the resulting effective normal stress, σ_n^{eff}, and the initial temperature, T_0, which is assumed to follow a geothermal gradient), the initial shear stress and the sliding velocity, as well as the tectonic loading rate. Both the configurations fail in the unstable regime, in that the ratio κ between the critical stiffness, $k_{\text{cr}} = (b - a)\sigma_n^{\text{eff}}/L$, and the machine stiffness, k, exceeds 1, so that the limiting

Table 1

Reference parameters adopted in this paper

Parameter	Value	
	Configuration A	Configuration B
Model parameters		
Loading velocity, v_{load}	3.17×10^{-10} m/s	1.17×10^{-9} m/s
Machine stiffness, k	10 MPa/m	7.5×10^{-2} MPa/m
Tectonic loading rate, $\dot{\tau}_0 = kv_{\text{load}}$	3.17×10^{-3} Pa/s	8.775×10^{-3} Pa/s
Vibration period of the analog freely slipping system, $T_{\text{a.f.}} = 2\pi\sqrt{m/k}$	5 s[a]	5 s[a]
Radiation damping constant, c (if present)	4.5 MPa s/m	2.86 MPa s/m
Critical velocity, v_c	1×10^{-4} m/s	1×10^{-4} m/s
Threshold velocity defining a seismic instability, v_l	0.1 m/s	0.1 m/s
Fault constitutive parameters		
Effective normal stress, σ_n^{eff}	30 MPa	100 MPa
Initial sliding velocity, v_0	3.17×10^{-10} m/s ($=v_{\text{load}}$)	1.17×10^{-9} m/s ($=v_{\text{load}}$)
Initial state variable, Ψ_0	3.15×10^{7} s ($=L/v_0$)	8.55×10^{6} s ($=L/v_0$)
Initial shear stress, τ_0	16.8 MPa ($=\mu_* \times \sigma_n^{\text{eff}}$)	65 MPa ($=\mu_* \times \sigma_n^{\text{eff}}$)
Initial temperature, T_0	483.15 K (=210 °C)	373.15 K (=100 °C)
Logarithmic direct effect parameter, a	0.008	0.010
Evolution effect parameter, b	0.016	0.014
Characteristic scale length, L	0.01 m	0.01 m
Critical stiffness, $k_{\text{cr}} = (b - a)\ \sigma_n^{\text{eff}}/L$	24 MPa/m	40 MPa/m
Reference value of the friction coefficient, μ_*	0.56	0.65
Reference value of the sliding velocity, v_*	3.17×10^{-10} m/s ($=v_0$)	1×10^{-6} m/s
Reference value of the temperature, T_*	210 °C ($=T_0$)	100 °C ($=T_0$)

The initial conditions (denoted by the subscript 0) refer to $t = 0$

[a] We do not change the period of the analog freely slipping system, because we are not interested in performing a stability analysis of the system

cycle is reached (Gu *et al*. 1984). As mentioned above, we emphasize that the limiting cycle can not be always reached if we include in the model additional complications, such as wear mechanism and thermal pressurization (see Bizzarri 2012b and references cite therein) or if we consider the Burridge-Knopoff (e.g., Erickson *et al*. 2011) with special parameters settings.

In order to explore whether the behavior at high speeds can influence the results, we have also considered the so-called frozen approximation of the friction law. In this approximation, the steady state friction becomes independent of the sliding velocity for speeds larger than a threshold value v_T (Weeks 1993; Bizzarri 2012c). In this case, the formulation of the RD law is expressed by Eq. (12); the counterparts for the DR and the CH can be derived in a straightforward way. In this paper, we also assume that $v_T = v_*$ (see Table 1); the results pertaining to the frozen simulations are reported as open symbols in the subsequent figures.

Finally, we have also considered the introduction of the radiation damping term (RDT thereinafter; Rice 1993; Beeler *et al*. 2001), which is known to control the dynamics of the system [Crupi and Bizzarri 2013; see Eq. (13)].

Overall, we have thoroughly explored the parameter space of both Configuration A and B, and we generated a synthetic catalog. From this catalog, we extracted the resulting cycle time (T_{cycle}). The latter, which is the limiting cycle of this system (e.g., Thompson and Stewart 2002), is determined as the time separating two subsequent instabilities: $T_{cycle}^{[n]} \underset{df}{=} t^{[n]} - t^{[n-1]}$ (see, among many other examples, Fig. 3 of Rice and Tse 1986) where $t^{[n]}$ is the time occurrence of the nth instability, which in turn is defined when the sliding speed exceeds a threshold value (v_l; see Table 1).

The aim of the present paper is not to perform a detailed analysis of the stability of the system. Indeed, the single mass-spring damped harmonic oscillator is described by a system of three nonlinear ordinary differential equations (ODEs), which have universal properties summarized in a very comprehensive way by Thompson and Stewart (2002). The body of the literature about the stability analysis of the spring-slider system is immense; among many others we cite here, the early studies of Gu *et al*. (1984) and Rice and Tse (1986), and the more recent generalizations of Ranjith and Rice (1999), Erickson *et al*. (2008), and Putelat *et al*. (2008, 2010, 2012). As stated above, we want the present work to be a contribution in the stream of papers dealing with the problem of the prediction of earthquake recurrence. In particular, we aim to explore whether it is possible, from a numerical and/or analytical point of view, to predict, in a deterministic way, the recurrence time of the next earthquake.

3. Numerical Results

3.1. Variation of a and b

In Fig. 1a, we plot the simulated cycle times depending on different values of the constitutive parameter a. We can clearly see that as long as a increases, T_{cycle} decreases with a linear pattern, and this holds for all the considered friction laws in the case of Configuration A (blue symbols). Remarkably, the slope of the T_{cycle} vs. a curve (namely, the ratio dT_{cycle}/da) is the same for a given friction law, but it changes if we consider a different set of parameters; this is apparent from the slope of the dashed lines. Moreover, that slope also depends on the adopted constitutive model; this is evident by comparing, for instance, the slope pertaining to the DR law (full blue squares), that pertaining to the RD law (full blue triangles) and that of the CH law (full blue circles). On the other hand, if we modify the frictional behavior at high speeds (i.e., if we include the frozen approximation), even for the same governing equation, the ratio dT_{cycle}/da changes. The same result holds for the DR and the RD if we also add the radiation damping term (RDT; small open squares and rectangles).

The behavior is quite different if we consider the CH law. Indeed, in the case of configuration B, we observe a net increase of T_{cycle} with increasing a (full red circles). On the other hand, the same behavior is obtained for configuration A if we consider the frozen approximation (open blue circles) and if we add the RDT (small open circles). To interpret this result, we have to remember that parameter a is responsible for

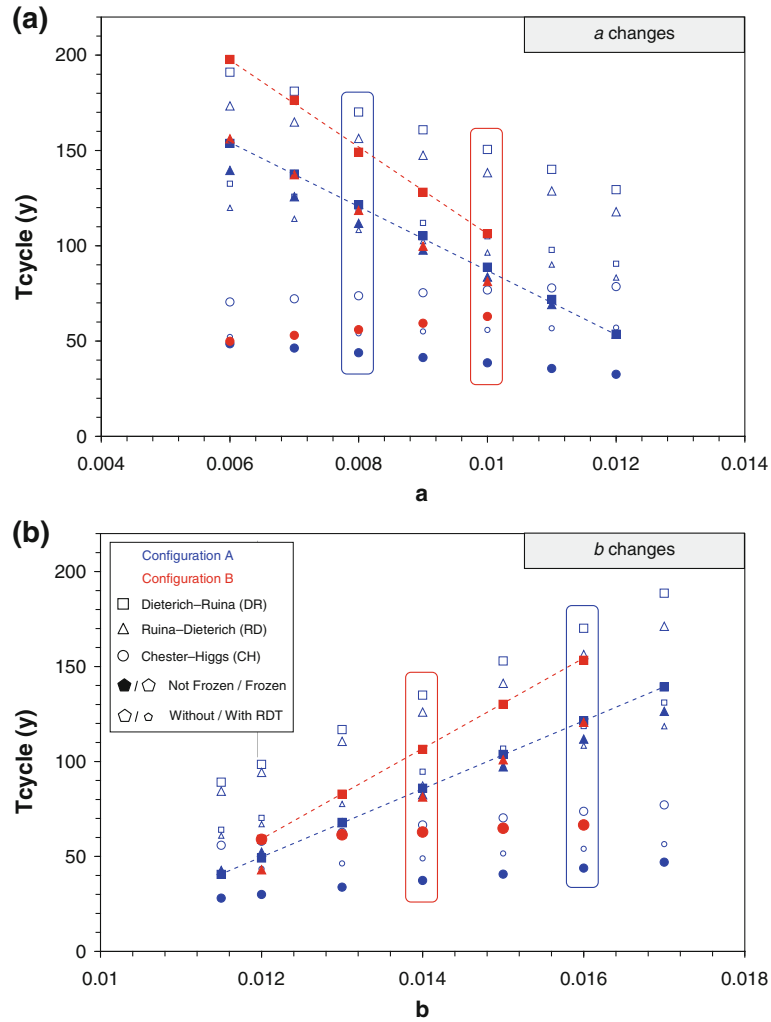

Figure 1

Cycle time (T_{cycle}) resulting by changing the constitutive parameters a [(panel (**a**)] and b [panel (**b**)]. All the other parameters are kept unchanged with respect to those listed in Table 1. *Blue symbols* refer to configuration A, while red symbols refer to configuration B. *Squares*, *triangles* and *circles* pertain to the Dieterich-Ruina [DR, Eq. (8)], Ruina-Dieterich [RD, Eq. (9)] and Chester-Higgs [CH, Eq. (10)] laws, respectively. *Empty symbols* denote numerical simulations where the frozen approximation at high speeds has been considered [see Eq. (12)]. Finally, *small symbols* indicate synthetic earthquakes in which the radiation damping term is included in the equation of motion [see Eq. (13)]. The *vertical rectangles* emphasize the reference set of parameters for both configuration A and configuration B

the so-called direct effect of friction, and it determines the amount of frictional stress that has to be exceeded in order to cause slip instability and thus the stress release (see also Bizzarri 2011b for a discussion). In the framework of the CH law, the frictional resistance depends explicitly on the temperature [see Eq. (10)], and this dependence is particularly relevant at sustained speeds. Once the slider tends to accelerate (so that the sliding speed becomes to be significant), the frictional heat starts to increase rapidly [see Eq. (11)], and its contribution to the value of the frictional resistance is not negligible. In other words, since the temperature affects the rupture threshold, the effect of the changes in a can be somehow masked by the overall dynamics of the system. A similar situation happens when we consider the parameter a varying explicitly with the temperature, so that $a = a(T)$ (Bizzarri 2012a).

This result suggests, even at this early stage of exploration of the parameter space, that it is very

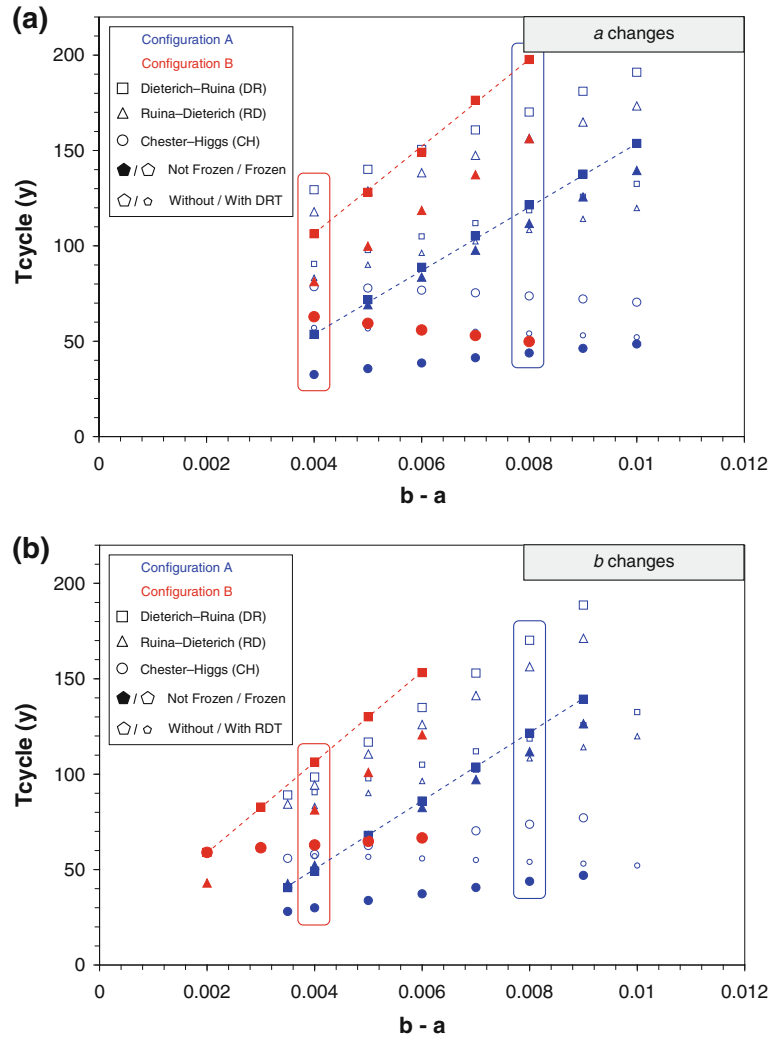

Figure 2
The same as in Fig. 1, but now we change the difference $b - a$. **a** Only the parameter a is changed. **b** Only the parameter b is changed

complicated to find an universal, analytical, empirical relationship expressing the value of the recurrence time as a function of the governing parameters, especially in the case of the CH friction model.

In Fig. 1b, the behavior of T_{cycle} for various b (and keeping all the other parameters as in Table 1) is plotted. Here we can see that, in general, T_{cycle} has a direct proportionality to b, for all the friction models (DR, RD and CH), configurations (A and B) and approximations (frozen or not, with and without the RDT). Nevertheless, the slope of the T_{cycle} vs. b curve (i.e., the ratio dT_{cycle}/db) is slightly different in the various cases, although it is constant for a given law and configuration (as emphasized by the dashed lines in Fig. 1b).

The results discussed above can be summarized by plotting T_{cycle} vs. the difference $b - a$; this is done in Fig. 2a (where only a is changed) and in Fig. 2b (where only b is changed). We know that recurrence time depends on the recovery time, i.e., on the time required to increase the traction from the friction level attained after a slip instability up to the upper yield stress, which defines the rupture point (the latter physically represents the maximum shear stress a fault can sustain by elastic deformations). The situation is described in Fig. 3 of Bizzarri and Crupi

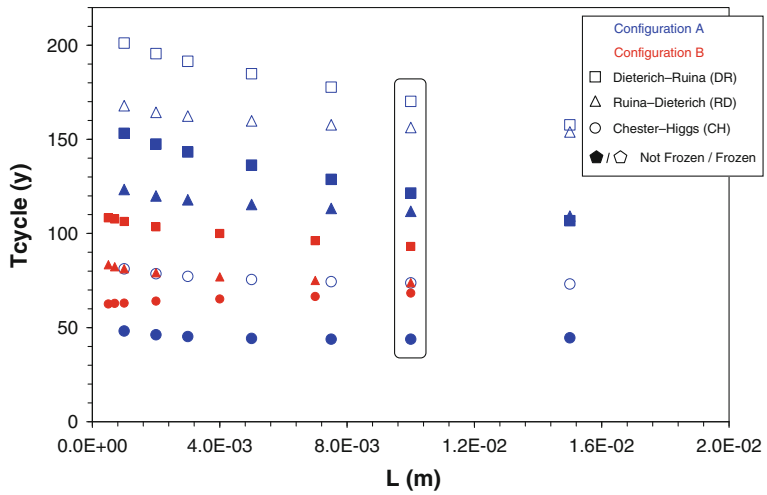

Figure 3
Behavior of T_{cycle} depending on the different values of the characteristic distance (L) controlling the evolution of the state variable. The *symbols* have the same meaning as in Fig. 1

(2013). Both the minimum and maximum traction depend on $b - a$, as also discussed by Bizzarri and Cocco [2003; see their Eqs. (12) and (13)]. Since the difference $b - a$ is directly proportional to the degree of instability of a fault [in other words, the greater $b - a$ is, the larger amount of stress is released; see also Gu and Wang (1991) and He *et al.* (2003)], we theoretically expect that the stress to be recovered during the interseismic fault restrengthening phase, which increases too, therefore leading to longer inter-event times. This general behavior emerges from Fig. 2, with the only exception of the CH law occurring when a is changed (see open blue and full red circles in Fig. 2a). This reflects exactly what we observe in Fig. 1a.

3.2. Variation of the Characteristic Length

The constitutive parameter L is the characteristic length scale appearing in the time evolution of the state variable. Physically, it represents the amount of slip over which the state variable Ψ evolves from one steady state to another (e.g., Ruina 1983). Moreover, it is related to the breakdown time (Bizzarri and Cocco 2003), which is spent during the process of the stress release (stress drop). Since the various governing models considered here have a different evolution law [see Eqs. (8)–(10)], we expect to have different values of the recurrence time even for the same value of L; this is exactly what we observe in Fig. 3, where we report the behavior of T_{cycle} for different L. With the exception of the CH for configuration B (full red circles), we can envisage from Fig. 3 a nearly linear decrease of T_{cycle} for increasing L. Contrary to what happens for variations of a and b, in the case of the variation of L, the introduction of the frozen approximation at high speeds does not change the slope of the T_{cycle} vs. L curve, but merely causes an increase of the recurrence time.

3.3. Variation of the Effective Normal Stress

Figure 4 reports the variations of T_{cycle} for varying σ_n^{eff}. The variation of the effective normal stress is associated with different focal depth and/or different values of the pore fluid pressure in the fault zone. It is clear that the dependence of the recurrence time on the effective normal stress is linear over a very broad range of compressive stresses. This behavior is a stable feature for both the configurations A and B and for all the considered friction laws. Also in this case, we can see that the introduction of the frozen approximation increases the value of T_{cycle}, but does not deface the linear dependence between the two quantities, although the slope of the T_{cycle} vs. σ_n^{eff} curve tends to increase if we include the frozen approximation. These results are consistent with the theoretical predictions; indeed, when σ_n^{eff} increases,

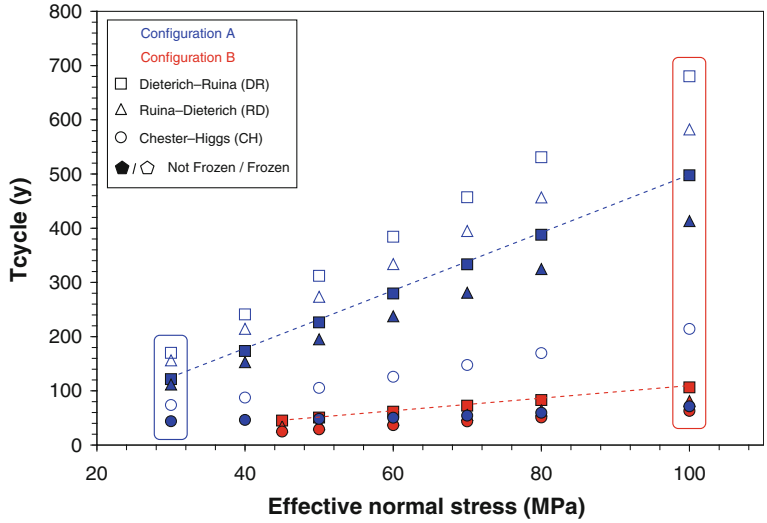

Figure 4
Behavior of $T_{\rm cycle}$, depending on the different values of the effective normal stress ($\sigma_n^{\rm eff}$). All the other parameters, including T_0 and T_*, are those tabulated in Table 1

the upper yield stress ($\tau_u^{\rm eq}$ in the naming convention of Bizzarri and Cocco 2003) also increases. At the same time, also the dynamic stress drop increases, because the fault becomes more unstable; we recall that although $\beta \equiv B/A$ remains constant by changing $\sigma_n^{\rm eff}$ ($B = b\sigma_n^{\rm eff}$ and $A = a\sigma_n^{\rm eff}$), the other parameter controlling the instability of the fault, $\kappa \equiv k_{\rm cr}/k$ (Bizzarri 2011a), increases for increasing $\sigma_n^{\rm eff}$. As a net result, the stress to be recovered after a dynamic instability in order to again reach the rupture point increases for increasing effective normal stress, thus leading to longer inter-event times.

An interesting issue is that the slope of the $T_{\rm cycle}$ vs. $\sigma_n^{\rm eff}$ curve strongly depends on the adopted governing model; in particular, for both the configurations A and B, the DR law is the model that is the most sensitive to variations of $\sigma_n^{\rm eff}$, while the CH model is the least sensitive.

3.4. Variation of the Loading Rate

The last dependence we explore is that of the loading rate. We change $\dot{\tau}_0$ by changing the value of the loading velocity ($v_{\rm load}$) and by keeping k (and thus κ) constant; this means that we do not change the rheological properties of the fault, but only the tectonic environment (i.e., the external conditions). Physically, we expect that the larger $\dot{\tau}_0$ is, the shorter $T_{\rm cycle}$ is. This makes sense, because when the loading force applied to the spring increases, then the interseismic recovery phase is faster (and correspondingly $T_{\rm cycle}$ is smaller). This expectation is verified from the results of our synthetic catalog, as depicted in Fig. 5, from which we can clearly appreciate an inverse dependence of $T_{\rm cycle}$ on $\dot{\tau}_0$. Remarkably, this holds for all the adopted governing laws, although, as for the dependence on $\sigma_n^{\rm eff}$, the DR law is the most sensitive to variations in $\dot{\tau}_0$, the CH is the least sensitive, and the RD is intermediate between the two. This is a stable feature for both configuration A and configuration B.

The dependence of $T_{\rm cycle}$ on $\dot{\tau}_0$ can be also understood from the analysis of the phase diagrams shown in Fig. 6. They refer to configuration B, but the results are qualitatively the same for Configuration A. We denote with the $\Delta\tau_{\rm rec}$ the amount of stress that the fault has to recover to again reach the rupture point (and thus cause a new slip instability). It is clear that as the loading rate increases, the resulting $\Delta\tau_{\rm rec}$ decreases, because, for the DR and the RD laws, the minimum sliding speed and the final level of friction increase, and because, at the same time, the upper yield stress decreases (Fig. 6a, b). Interestingly, in the case of the CH (Fig. 6c) the opposite holds, in that as

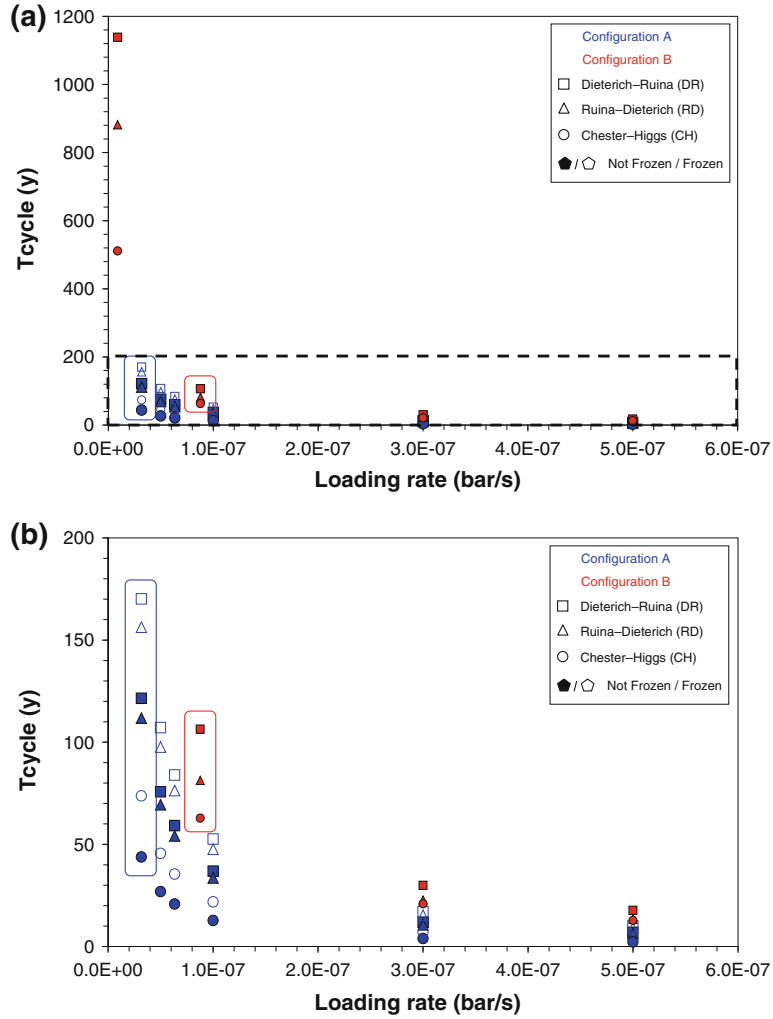

Figure 5
Behavior of T_{cycle} depending on the different values of the loading rate ($\dot{\tau}_0$). In panel (**b**), we expand the *dashed region* marked in panel (**a**)

$\dot{\tau}_0$ increases, the minimum sliding speed and the final level of friction decrease, but the upper yield stress increases. As observed previously, this "anomalous" behavior (if compared to the DR and the RD law) is imputable to the explicit dependence of friction on developed temperature. The net result for the CH law is that $\Delta\tau_{rec}$ decreases for increasing $\dot{\tau}_0$, but more slowly than in the case of DR and RD laws.

4. Discussion

In this paper, we have considered a single-degree-of-freedom mass-spring analog fault system (1-D) to investigate whether it is possible to express the recurrence time of earthquakes (T_{cycle}) through an universal, analytical equation depending on the constitutive properties of the seismogenic structure. This amenable picture requires some caveats. First of all, we emphasize that the concept itself of the cycle time (or limiting cycle) can somehow be misleading; indeed, as discussed by Bizzarri (2012b) and in Sect. 1, some different mechanisms can take place during faulting, affecting the overall dynamics of the seismogenic structure and therefore making the concept of T_{cycle} even meaningless. In idealized conditions, it is well known that a velocity-weakening 1-D system will reach its limiting cycle (e.g., Gu

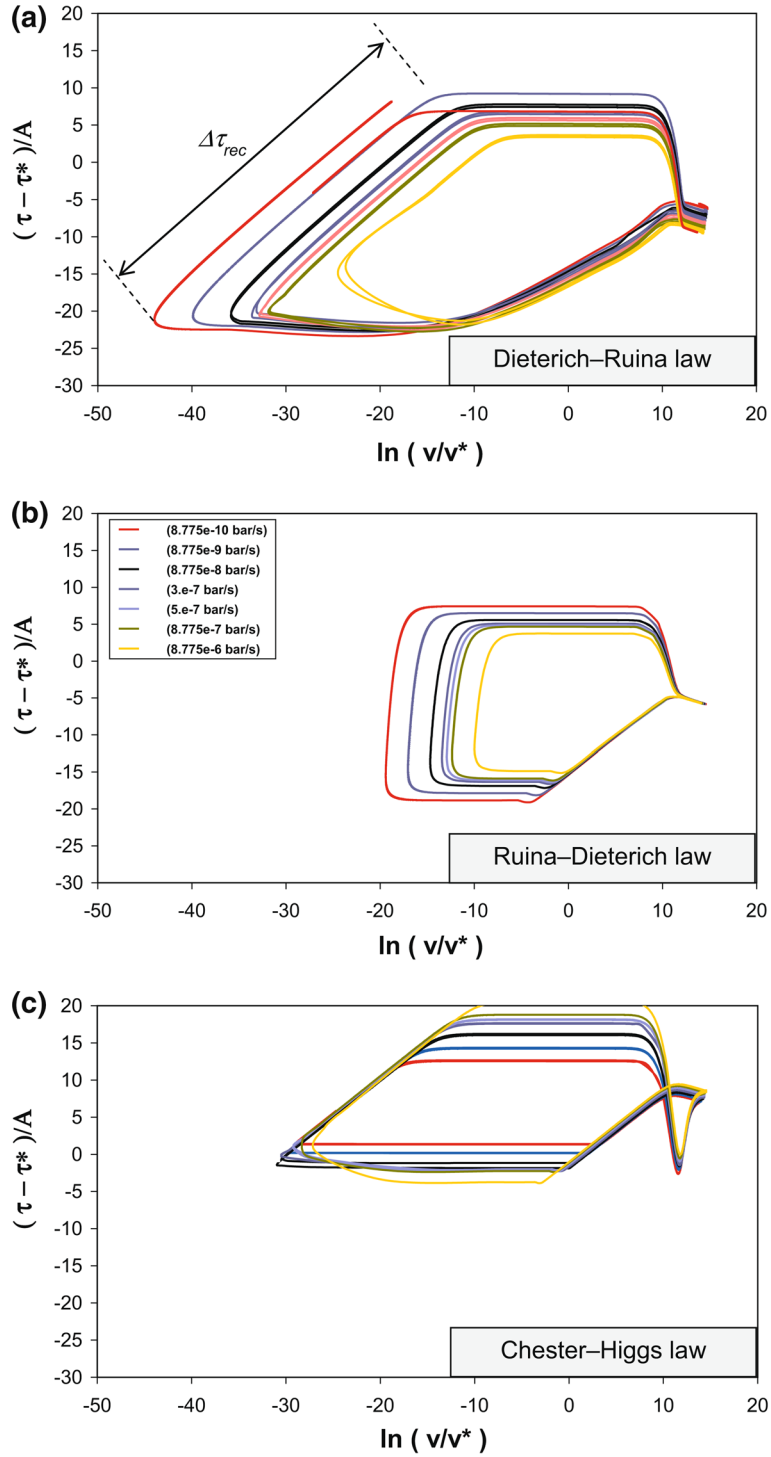

Figure 6
Phase diagrams in the case of configuration B for various values of the loading rate. **a** Orbits for the DR law, which correspond to the full *red squares* of Fig. 5a. **b** Orbits for the RD law, which correspond to the full red triangles of Fig. 5a. **c** Orbits for the CH law, which correspond to the full *red circles* of Fig. 5a. All the quantity are normalized; τ_* and v_* are references values for the shear stress and the sliding velocity, respectively

et al. 1984, among many others), which is characterized by the same recurrence time, because the states of the dynamical system (expressed in terms of sliding speed and shear stress) are defined by a limiting orbit in the phase space (i.e., the limiting cycle; see Thompson and Stewart 2002). This behavior mathematically expresses the concept of the characteristic earthquake (CE; Reid 1910). This simplistic (and idealized) picture is dramatically altered if we account for possible phenomena, such as stress triggering and fault interaction, wear processes on the fault core, permeability and porosity evolution, etc. (Bizzarri 2012b). Practically, these phenomena can impede the fault from reaching its limiting cycle, so that T_{cycle} can not be determined, but this intimately depends on the actual state of the fault (which is usually unknown for natural faults).

Another important point is inherently related to the choice of the analog fault model. As pointed out earlier by Rice and Tse (1986), the single mass-spring model is certainly oversimplified, in that it predicts that an asperity fails once it reaches its critical state; indeed, we can expect that at natural conditions some patches on the fault can reach the failure point and nucleate the rupture. Moreover, the spring-slider model exhibits only a dependence on time, implying that all the properties of the fault are spatially homogeneous and that they can be represented, in an average sense, by the adopted values of the constitutive parameters. Indeed, the role of spatial heterogeneities in the fault rheology are important in the whole dynamic of a seismic fault zone (e.g., Oglesby and Day 2002; Tinti *et al*. 2005; Ampuero *et al*. 2006; Ripperger *et al*. 2008; Bizzarri *et al*. 2010; Song and Sommerville 2010). Therefore, the single spring-slider model can only be regarded as a first approximation of the behavior of a real-world fault. Indeed, since it naturally represents the stick-slip mechanism, it has been successfully employed to study the traction evolution on a seismic fault and to simulate repeated earthquake events (Boatwright and Cocco 1996; Beeler *et al*. 2001; Bizzarri 2010; Mitsui and Cocco 2010 among many others). As pointed out by Bizzarri and Belardinelli (2008), the agreement between results from a single spring-slider model and from an continuum, extended (3-D) fault model is excellent during the slow nucleation phase; during the subsequent acceleration phase, in a given fault point, the 3-D model experiences the contribution of the stress redistribution on the fault (i.e., of the load due to the neighboring points that are already slipping and releasing stress). This phenomenon is obviously neglected in the single spring-slider model. We also mention here the comparison performed by Weatherley and Abe (2004) between a 1-D chain of mass-block models and a lattice solid model.

Given these significant limitations, we have considered here the most simple situation in which the system reaches the limiting cycle; in such a situation, the system forgets the initial conditions ($t = 0$). In this case, which represents the CE model, we can write (see also Barbot *et al*. 2012):

$$T_{\text{cycle}} = \frac{\Delta\tau_{\text{rec}}}{\dot{\tau}_0} \tag{1}$$

The inverse proportionality between stress drop and loading velocity (recall that the tectonic loading rate equals $k\ v_{\text{load}}$) and the direct proportionality between recurrence intervals and stress drop have been previously shown in the case of the RD law by Cao and Aki (1986) and Gu and Wang (1991) and extended to the DR model by He *et al*. (2003).

In the framework of the rate-dependent and state-dependent friction laws, both the maximum yield stress (τ_u^{eq}) and the dynamic stress drop [$\Delta\tau_d$; see Eq. (12) of Bizzarri 2012b] are a priori unpredictable (Bizzarri 2003). This translates into the fact that $\Delta\tau_{\text{rec}}$ can not be predicted exactly a priori.

By adopting two rather different configurations (see Table 1), and by adopting three different governing models (the Dieterich-Ruina (DR), the Ruina-Dieterich (RD) and the Chester-Higgs (CH) laws; see Appendix A), we have generated a synthetic catalog of nearly 500 different seismic sequences.

Our simulations clearly confirm for all the adopted governing equations (including the CH model, the frozen versions of governing laws and with the RDT) the inverse proportionality between T_{cycle} and $\dot{\tau}_0$ stated by Eq. (1) (see Fig. 5), which is relatively obvious from a physical point of view. Moreover, our numerical results suggest, in general, the following dependencies:

$$T_{\rm cycle} \propto b - a \tag{2}$$

(see Fig. 2),

$$T_{\rm cycle} \propto \sigma_n^{\rm eff} \tag{3}$$

(see Fig. 4), and

$$T_{\rm cycle} \propto -L \tag{4}$$

(see Fig. 3).

The dependencies we found in Eqs. (2) and (3) confirm the results that Gu and Wang (1991) and He *et al*. (2003) obtained for the canonical formulations (i.e., without frozen and without RDT) of the RD and DR models, respectively. Indeed, they found [see Eq. (4) in Gu and Wang 1991] that

$$\Delta\tau_{\rm rec} = (b-a)\,\sigma_n^{\rm eff}\left[K - \zeta \ln\left(\frac{v_{\rm load}}{v_*}\right)\right] \tag{5}$$

where K is a parameter with an inverse proportionality with $1/\kappa$ and having a weak dependence on m and $\zeta \approx 2$. Remarkably, Gu and Wang (1991) and He *et al*. (2003) do not consider the dependence of $\Delta\tau_{\rm rec}$ (and thus of $T_{\rm cycle}$) on L.

Lapusta *et al*. (2012) and Barbot *et al*. (2012), in order to fit the recurrence times of the Parkfield segment of the San Andreas fault with the DR friction law, proposed the following analytical relation:

$$T_{\rm cycle} = \frac{(b-a)\,\sigma_n^{\rm eff}}{\dot{\tau}_0} \ln\left(\frac{v_{\rm co}}{v_{\rm inter}}\right) \tag{6}$$

where $v_{\rm co}$ is a coseismic values of the fault slip velocity (they use $v_{\rm co} = 1$ m/s) and $v_{\rm inter}$ is the interseismic fault slip velocity (they use $v_{\rm inter} = 1 \times 10^{-12}$ m/s, so that the correcting, non-dimensional factor $\ln\left(\frac{v_{\rm co}}{v_{\rm inter}}\right)$ equals 27.63). The parameters of Eq. (6) have been tuned in order to reproduce a posteriori the observed recurrence times at Parkfield. We note that Eq. (6) has been derived by assuming that the stress drop between two subsequent instabilities can be determined analytically in terms of the governing parameters and of the two velocities $v_{\rm co}$ and $v_{\rm inter}$.

In general, $\sigma_n^{\rm eff}$ can somehow be estimated, based on the representative hypocentral depth of a seismogenic zone, and $\dot{\tau}_0$ can be inferred from geological and seismotectonic observations. However, from a predictive point of view, Eq. (6) has some problems, in that it is very difficult to a priori constraint the values of $v_{\rm co}$ and $v_{\rm inter}$; both of them are known to vary over several orders of magnitude, especially $v_{\rm inter}$ (see for instance Fig. 6, from which is it clear the high variability of the sliding speeds attained during the interseismic phase). Moreover, it is also known that $v_{\rm co}$ can be higher than 1 m/s; for instance, the thermal pressurization of pore fluids, the flash heating of micro-asperity contacts (and in general every mechanism causing a dramatic fault weakening) are usually associated with very high values of coseismic slip peak (see for instance Bizzarri 2012a). We emphasize that a variation of a factor of 10 in $\frac{v_{\rm co}}{v_{\rm inter}}$—very common in numerical simulations—causes a variation roughly of 8 % in $T_{\rm cycle}$. Incidentally, we mention here that if we ad hoc tune the values of $\frac{v_{\rm co}}{v_{\rm inter}}$ differently for all the set of parameters used in the DR models, we can adequately reproduce the observed cycle time with Eq. (6), but we emphasize that his tuning is done a posteriori and without any physical or observational constraints.

Moreover, Eqs. (6)— and (5) as well—do not explicitly incorporate the dependence on the characteristic distance L, which controls the evolution of the state variable, and which, although small, cause variations of $T_{\rm cycle}$ (see Fig. 3).

In the framework of the rate-dependent and state-dependent friction laws, the dynamic stress drop can be associated with the difference $b - a$ (e.g., Ruina 1983; Gu *et al*. 1984; Gu and Wang 1991; He *et al*. 2003, among many others). However, we have seen that it is extremely difficult to a priori predict the two states in the phase plane which determine $\Delta\tau_{\rm rec}$ (i.e., the minimum in (v, τ) and the upper yield stress), and therefore it is hard to exploit Eq. (1) in order to give a quantitative prediction of the recurrence time. This is particularity true in the case of the CH law, for which the explicit dependence on temperature complicates, with respect to the DR and the RD laws, the traction evolution at high speeds. More explicitly, temperature evolution controls the rupture point (i.e., the upper yield stress level), the dynamic stress release and the final level of friction (and thus the level of friction at which the long-stage interseismic phase begins).

5. Conclusions

The quantitative determination of the recurrence time of an earthquake definitively remains one of the most pursued objectives in seismology. It has been already demonstrated that the concept of recurrence time itself can be misleading or even meaningless, in that many causes can alter the idealized cyclic behavior postulated by the theory of characteristic earthquakes (CE; see the discussion on Bizzarri 2012b).

At a fundamental level, in addition to statistical inferences (i.e., probabilistic predictions), which are disregarded here, there are analytical and numerical predictions of the recurrence of a next earthquake. The former can be ideally retrieved theoretically, or empirically inferred from data. The latter is a result of a specific numerical experiment, where the physics of the fault, as well as all the parameters of the model, are assumed to be known.

The laboratory-derived, macroscopic theory of the rate-dependent and state-dependent friction laws provides a framework in which the whole life of a seismogenic structure can be modeled, and thus the cycle time can be calculated. In this framework, by using a 1-D spring-slider dashpot model and neglecting all possible phenomena that can cause deviations from the CE model, we have generated a synthetic catalog of nearly 500 different seismic sequences, by considering a large class of fault governing models and approximations. Through a systematic exploration of the parameter space, we confirm that T_{cycle} is directly proportional to the recovery stress ($\Delta\tau_{\mathrm{rec}}$; e.g., Fig. 6a) and inversely proportional to the loading rate ($\dot{\tau}_0$; see Fig. 5); see Eq. (1). We also found a linear, positive dependence of T_{cycle} on the effective normal stress [σ_n^{eff}; see Fig. 4 and Eq. (3)], previously found in some cases. Moreover, our numerical experiments indicate a linear, negative dependence of T_{cycle} on the characteristic distance [L; see Fig. 3 and Eq. (4)]. Remarkably, these dependences hold for all the governing models considered here, the Dieterich-Ruina (DR), the Ruina-Dieterich (RD) and the Chester-Higgs (CH) laws, and also with the frozen approximation and or with the RDT. Our study therefore generalizes previous findings by Gu and Wang (1991) and He *et al.* (2003).

One of the major outcome of the present study is that the proportionality coefficients strongly depend on the specific form of the adopted constitutive model, on its behavior at high speeds and on the possible introduction of the radiation damping term (mimicking the energy lost as radiated seismic waves).

Moreover, we also found that the positive proportionality between T_{cycle} and the difference $b - a$, confirmed in general for DR and RD laws, does not hold for the CH law in some cases (see Fig. 2). This difference is basically attributed to the effect of the temperature developed by frictional heat, which directly controls the evolution of traction in the CH case, because it is incorporated explicitly in the governing equations.

As an overall conclusion, although our catalog is qualitatively compatible with previous relations inferred for the RD by Lapusta and Barbot (2012); (see also Barbot *et al.* 2012) in the case of the DR and the RD laws, the exact, a priori determination of the recurrence time (through an universal, analytical equation) is very complicated, even in the simplest (and idealized) case of the CE model. This is because the proportionality coefficients depend on the adopted friction law and on the global set of model parameters (just as an example, from Fig. 4 we have that the slope of the T_{cycle} vs. σ_n^{eff} curve for the DR is significantly different from configuration A to configuration B). The a priori prediction, again through a unique equation, of the recurrence time is virtually impossible if we postulate that the traction evolution of the fault is described by the CH law; in such a case, we can even invert the proportionality relation observed for the other two friction models (see Fig. 2).

To conclude, we have shown that, even in the simplest case of the CE models considered here, the belief that it is possible to predict the recurrence time of a next earthquake through an universal, *analytical*, empirical equation is not supported by numerical evidence. Indeed, the results presented here can provide some general guidance about how the recurrence intervals can depend on the adopted model parameters.

As mentioned above, there is another approach to try to predict (still in a deterministic framework) the

recurrence time. Numerical simulations (such as those performed here or even with more elaborated models, such a Burridge-Knopoff or continuum models) should enable us to have a *numerical* estimate of a subsequent earthquake. But the problem here is that, in spite of significant advances in the understanding of the plate tectonics and fault structures, we currently know little about the stress state in the Earth (initial and external conditions) and about the most proper friction law that can describe a given earthquake sequence (earthquake source physics). Moreover, we have to exactly know the values of the governing parameters (input data in the forward models), which are often not so well constrained by independent observation or can even change through time (i.e., during the whole life of the fault), making the problem highly nonlinear.

From another point of view, it might be emphasized that recurrence intervals are not the best way to infer the frictional properties of a given seismogenic structure, because we do not know if the available fault constitutive models are adequate to describe the whole life of that fault, or simply which is the best one among the various possibilities. However, variations in stress drop in repeating earthquakes can give some indication on the healing rate (e.g., Marone 1998; Marone *et al*. 1995), which becomes dominant once the fault has slowed significantly. At the same time, the analysis of repeating slip failures are used to constrain the loading rate (e.g., Nadeau and McEvilly 1999; Igarashi *et al*. 2003).

The present exercise falls in the stream of papers dealing with the earthquake prediction, and can be regarded as a possible, although preliminary, way to connect the source physics to the earthquake prediction.

Acknowledgments

The first author (A.B.) thanks the editors of this topical volume, A. Oth, K. Mayeda and L. Rivera, for having invited him to contribute, and G. F. Panza for some discussions on the general topic of earthquakes prediction. The guest editor, A. Oth, and three anonymous referees are acknowledged for their stimulating comments and criticism, which contributed to improvements to the paper.

Appendix: Numerical Details of the Model and Constitutive Equations

In this section, we briefly recall all the equations adopted in the present study. Readers can refer to the cited references for a more verbose discussion of the equations.

As mentioned in Sect. 2, we use here the single-degree-of-freedom (1-D) spring-slider analog fault model. The equation of motion of such a system is that of an harmonic oscillator (far of being exhaustive, we mention here Gu *et al.* 1984; Gu and Wang 1991; He *et al*. 2003; Ranjith and Rice 1999):

$$m\ddot{u} = k(u_{load} - u) - \tau \tag{7}$$

in which the overdots indicate the time derivative, m is the mass per unit surface, k denotes the elastic constant of the spring (which mimics the elastic behavior of the medium surrounding the fault), u_{load} is the displacement of the loading point (which moves at the prescribed velocity $v_{\mathrm{load}} \equiv \dot{u}_{\mathrm{load}}$), u is the displacement and τ is the frictional resistance acting of the sliding surface. As described in the following, the choice of the analytical expression of τ defines the adopted governing model. The elastodynamic problem for our 1-D fault system is solved numerically by using the fourth-order Runge-Kutta algorithm with auto-adaptive time stepping (Press *et al*. 1992).

The single mass-spring system is an obvious simplification of the more elaborated Burridge-Knopoff model (see Burridge and Knopoff 1964; Carlson and Langer 1989a, b; Carlson *et al.* 1991; Erickson *et al*. 2011, among many others), where multiple masses are connected with springs. This inherently discrete fault model can account for spatial heterogeneities and it is a first step toward the continuum finite difference or finite element models.

In the present paper, we use various governing laws; the Dieterich-Ruina model (Dieterich 1978, 1994):

$$\begin{cases} \tau = \left[\mu_* + a\ln\left(\frac{v}{v_*}\right) + b\ln\left(\frac{\psi v_*}{L}\right)\right]\sigma_n^{\mathrm{eff}} \\ \frac{\mathrm{d}}{\mathrm{d}t}\psi = 1 - \frac{\psi v}{L} \end{cases} \tag{8}$$

the Ruina-Dieterich model (Ruina 1983; Marone 1998):

$$\begin{cases} \tau = \left[\mu_* + a\ln\left(\frac{v}{v_*}\right) + b\ln\left(\frac{\psi v_*}{L}\right)\right]\sigma_n^{eff} \\ \frac{\mathrm{d}}{\mathrm{d}t}\psi = -\frac{\psi v}{L}\ln\left(\frac{\psi v}{L}\right) \end{cases} \quad (9)$$

and the Chester-Higgs model (Chester and Higgs 1992; Chester 1994):

$$\begin{cases} \tau = \left[\mu_* + a\ln\left(\frac{v}{v_*}\right) + b\ln\left(\frac{\Psi v_*}{L}\right) + \frac{aQ_a}{R}\left(\frac{1}{T} - \frac{1}{T_*}\right)\right]\sigma_n^{\mathrm{eff}} \\ \frac{\mathrm{d}}{\mathrm{d}t}\Psi = -\frac{\Psi v}{L}\left[\ln\left(\frac{\Psi v}{L}\right) + \frac{Q_b}{R}\left(\frac{1}{T} - \frac{1}{T_*}\right)\right] \end{cases} \quad (10)$$

In Eqs. (8)–(10) v is the sliding velocity, Ψ is a state variable (an empirical variable accounting for the previous sliding history of the system and usually interpreted as the average characteristic lifetime of contacting asperities; Marone 1998; Ruina 1983), a, b and L are the constitutive parameters, μ_* and v_* are reference values of the friction coefficient and sliding velocity, respectively (namely, μ_* is the steady state value of the friction coefficient when the sliding velocity equals v_*) and σ_n^{eff} is the effective normal stress (assumed constant through time in the present modeling). In Eq. (10) Q_a and Q_b are apparent activation energies (we use $Q_a = Q_b = 1 \times 10^5$ J/mol as in Chester 1994), R is the universal gas constant, T is the (absolute) temperature produced by frictional heat and T_* is a (absolute) reference temperature value. T is computed as follows (McKenzie and Brune 1972; Kato 2001; Bizzarri and Crupi 2013):

$$T(t) = T_0 + \frac{1}{2C\sqrt{\pi\chi}}\int \frac{\tau(t')\,v(t')}{\sqrt{t - t'}}\,dt' \quad (11)$$

in which T_0 is the (absolute) initial temperature, C is the heat capacity of the bulk composite for unit volume [we use $C = 3 \times 10^6$ J/(m^3 K)], χ is the thermal diffusivity (we use $\chi = 1 \times 10^{-6}$ m^2/s) and t is time.

To perform a more comprehensive comparison of the various governing models that can be used to describe the traction evolution, we also consider a modification of the canonical rate-dependent and state-dependent friction laws, where the steady state friction (defined as the friction when the state variable is constant through time, i.e., when $\frac{\mathrm{d}}{\mathrm{d}t}\Psi = 0$) becomes independent on the sliding velocity at high speeds. Namely, for v greater than a threshold value v_{T} the Ruina-Dieterich model (10) becomes:

$$\begin{cases} \tau = \left[\mu_* + a\ln\left(\frac{v_{\mathrm{T}}}{v_*}\right) + b\ln\left(\frac{\psi v_*}{L}\right)\right]\sigma_n^{\mathrm{eff}} \\ \frac{\mathrm{d}}{\mathrm{d}t}\psi = -\frac{\psi v}{L}\ln\left(\frac{\psi v_{\mathrm{T}}}{L}\right) \end{cases} \quad (12)$$

This modification, basically due to Weeks (1993), comes from the laboratory inferences of Scholz and Engelder (1976) and Dieterich (1978).

Finally, we consider a modification of the equation of motion (7), where the so-called radiation damping term (RDT) is introduced (Xu and Knopoff 1994; Beeler 2001, 2006; Beeler *et al.* 2002; Crupi and Bizzarri 2013),

$$m\ddot{u} = k(u_{load} - u) - \tau - cv \quad (13)$$

where

$$c \equiv \frac{G}{2\,v_{\mathrm{S}}} \quad (14)$$

with G being the rigidity of the elastic medium and v_S the S wave velocity away from the fault plane. Physically, the radiation damping approximation (Rice 1993) mimics the energy lost due to seismic wave propagation, which is inherently present continuum fault models.

References

Allen, R. M. (2007), Earthquake hazard mitigation: New directions and opportunities, In: Treatise on Geophysics (G. Schubert Ed.). 4—Earthquake seismology (H. Kanamori Ed.), 607–648, Elsevier, doi:10.1016/B978-044452748-6/00083-3.

Ampuero, J.-P., Ripperger, J., and P. M. Mai (2006), Properties of dynamic earthquake ruptures with heterogeneous stress drop, in *Radiated Energy and the Physics of Earthquakes*, Abercrombie, R., A. McGarr, H. Kanamori, and G. di Toro (Editors), Geophys. Monogr., *170*, American Geophysical Union, Washington, DC., 255–261.

Barbot, S., Lapusta, N., and J.-P. Avouac (2012), Under the hood of the earthquake machine: Toward predictive modeling of the seismic cycle, Science, *336*, 707–710.

Beeler, N. M. (2001), Stress drop with constant, scale independent seismic efficiency and overshoot, Geophys. Res. Lett., *28*, No. 17, 3353–3356.

Beeler, N. M. (2006), Inferring earthquake source properties from laboratory observations and the scope of lab contributions to source physics, In Radiated Energy and the Physics of Faulting, Abercrombie, R., A. McGarr, H. Kanamori, and G. di Toro (Editors), Geophys. Monogr., *170*, American Geophysical Union, Washington, DC., 99–119.

Beeler, N. M., Hickman, S. H., and T.-F. Wong (2001), Earthquake stress drop and laboratory-inferred interseismic strength recovery, J. Geophys. Res., *106*, No. B12, 30,701–30,713.

Beeler, N. M., Wong, T.-F., and T. E. Tullis (2002). Slip-weakening distance and fracture energy during dynamic sliding with laboratory-inferred fault strength, Proc. 2002 SCEC Meeting, Oxnard, CA.

Bizzarri, A. (2010), On the recurrence of earthquakes: Role of wear in brittle faulting, Geophys. Res. Lett., *37*, L20315, doi:10.1029/2010GL045480.

Bizzarri, A. (2011a), Temperature variations of constitutive parameters can significantly affect the fault dynamics, Earth Plan. Sci. Lett., *306*, 272–278, doi:10.1016/j.epsl.2011.04.009.

Bizzarri, A. (2011b), On the deterministic description of earthquakes, Rev. Geophys., *49*, RG3002, doi:10.1029/2011RG000356.

Bizzarri, A. (2012a), Rupture speed and slip velocity: What can we learn from simulated earthquakes?, Earth Plan. Sci. Lett., *317–318*, 196–203, doi:10.1016/j.epsl.2011.11.023.

Bizzarri, A. (2012b), What can physical source models tell us about the recurrence time of earthquakes?, Earth–Science Reviews, *115*, 304–318, doi:10.1016/j.earscirev.2012.10.004.

Bizzarri, A. (2012c), Formulation of a fault governing law at high sliding speeds: Inferences from dynamic rupture models, Earth Plan. Sci. Lett., *355–356*, 223–230, doi:10.1016/j.epsl.2012.09.007.

Bizzarri, A., and M. E. Belardinelli (2008), Modelling instantaneous dynamic triggering in a 3–D fault system: application to the 2000 June South Iceland seismic sequence, Geophys. J. Int., *173*, 906–921, doi:10.1111/j.1365-246X.2008.03765.x.

Bizzarri, A., and M. Cocco (2003), Slip–weakening behavior during the propagation of dynamic ruptures obeying rate– and state–dependent friction laws, J. Geophys. Res., *108*, No. B8, 2373, doi:10.1029/2002JB002198.

Bizzarri, A., and Crupi, P. (2013), Is the initial thermal state of a fault relevant to its dynamic behavior?, Bull. Seism. Soc. Am., *100*, No. 3, 2062–2069, doi:10.1785/0120120279.

Bizzarri, A., Dunham, E. M., and P. Spudich (2010), Coherence of Mach fronts during heterogeneous supershear earthquake rupture propagation: Simulations and comparison with observations, J. Geophys. Res., *115*, B08301, doi:10.1029/2009JB006819.

Boatwright, J., and M. Cocco (1996), Frictional constraints on crustal faulting, J. Geophys. Res., *101*, No. B6, 13,895–13,909, doi:10.1029/96JB00405.

Burridge, R., and L. Knopoff (1964), Body force equivalents for seismic dislocations, Bull. Seismol. Soc. Am., *54*, 1875–1888.

Cao, T., and K. Aki (1986), *Seismicity simulation with a rate- and state-dependent fricion law*, Pure Appl. Geophys., *124*, No. 3, 487–513.

Carlson, J. M., and J. S. Langer (1989a), Properties of earthquakes generated by fault dynamics, Phys. Rev. Lett., *62*, 2632–2635, doi:10.1103/PhysRevLett.62.2632.

Carlson, J. M., and J. S. Langer (1989b), A mechanical model of an earthquake fault, Phys. Rev. A, *40*, 6470–6484, doi:10.1103/PhysRevA.40.6470.

Carlson, J. M., Langer, J. S., Shaw, B. E. and C. Tang (1991), Intrinsic properties of a Burridge–Knopoff model of an earthquake fault, Phys. Rev. A, *44*, No. 2, 884–897.

Chester, F. M. (1994), Effects of temperature on friction: Constitutive equations and experiments with quartz gouge, J. Geophys. Res., *99*, 7247–7261, doi:10.1029/93JB03110.

Chester, F. M. and H. G. Higgs (1992). Multimechanism friction constitutive model for ultrafine quartz gouge at hypocentral conditions, J. Geophys. Res., *97*, B2, 1859–1870.

Crupi, P., and Bizzarri, A. (2013), The role of radiation damping in the modeling of repeated earthquake events, Ann. Geophys., *56*, No. 1, R0111, doi:10.4401/ag-6200.

Dieterich, J. H. (1978), Time–dependent friction and the mechanics of stick slip, Pure Appl. Geophys., *116*, 790–806, doi:10.1007/BF00876539.

Dieterich, J. H. (1994), A constitutive law for rate of earthquake production and its application to earthquake clustering, J. Geophys. Res., *99*, No. B2, 2601–2618.

Erickson, B., Birnir, B., and D. Lavallée (2008), *A model for aperiodicity in earthquakes*, Nonlin. Proc. Geophys., *15*, 1–12.

Erickson, B. A., Birnir, B., and D. Lavallée (2011), Periodicity, chaos and localization in a Burridge–Knopoff model of an earthquake with rate–and–state friction, Geophys. J. Int., *187*, 178–198, doi:10.1111/j.1365-246X.2011.05123.x.

Gu, J. C., Rice, J. R., Ruina, A. L., and S. T. Tse (1984), Slip motion and stability of a single degree of freedom elastic system with rate and state dependent friction, J. Mech. Phys. Sol., *32*, 167–196, doi:10.1016/0022-5096(84)90007-3.

Gu, Y., and T. -f. Wong (1991), Effects of loading velocity, stiffness, and inertia on the dynamics of a single degree of freedom spring–slider system, J. Geophys. Res., *96*, No. B13, 21,677–21,691.

He, C., Wong, T. -f., and N. M. Beeler (2003), Scaling of stress drop with recurrence interval and loading velocity for laboratory-derived fault strength relations, J. Geophys. Res., *108*, 2037, doi:10.1029/2002JB001890.

Heisenberg, W. (1927), Über den anschaulichen Inhalt der quantentheoretischen kinematik und mechanik, Zeitschrift für Physik, *43*, Nos. 3–4, 172–198.

Igarashi, T., Matsuzawa, T., and A. Hasegawa (2003), Repeating earthquakes and interplate aseismic slip in the northeastern Japan subduction zone, J. Geophys. Res., *108*, No. B5, doi:10.1029/2002JB001920.

Kossobokov, V. G., and A. K. Nekrasova (2012), Global seismic hazard assessment program maps are erroneous, Seismic Instruments, *48*, No. 2, 162–170.

Kato, N. (2001). Effect of frictional heating on pre-seismic sliding: a numerical simulation using a rate-, state- and temperature-dependent friction law, Geophys. J. Int., *147*, 183–188.

Lapusta, N., and S. Barbot (2012), Models of earthquakes and aseismic slip based on laboratory–derived rate and state friction laws, In: The Mechanics of Faulting: From Laboratory to Real Earthquakes (A. Bizzarri and H. S. Bhat Eds.), Research Signpost, ISBN 978-81-308-0502-3.

Marone, C. J. (1998), The effect of loading rate on static friction and the rate of fault healing during the earthquake cycle, Nature, *391*, 6662, 69–72.

Marone, C. J., Vidale, J. E., and W. L. Ellsworth (1995), Fault healing inferred from time dependent variations in source properties of repeating earthquakes, Geophys. Res. Lett., *22*, No. 22, 3095–3098, doi:10.1029/95GL03076, 1995.

McKenzie, D., and J. N. Brune (1972). Melting on fault planes during large earthquakes, Geophys. J. R. Astr. Soc., *29*, 65–78.

Mitsui, Y., and M. Cocco (2010), The Role of porosity evolution and fluid flow in frictional instabilities: A parametric study using a spring–slider dynamic system, Geophys. Res. Lett., *37*, L23305, doi:10.1029/2010GL045672.

Nadeau, R. M., and T. V. McEvilly (1999), Fault slip rates at depth from recurrence intervals of repeating microearthquakes, Science, *285*, No. 5428, 718–721, doi:10.1126/science.285.5428.718.

Oglesby, D. D., and S. M. Day (2002), Stochastic fault stress: Implications for fault dynamics and ground motion, Bull. Seismol. Soc. Am., *92*, 3006–3021.

Panza, G. F., Romanelli, F., and F. Vaccari (2001), Seismic wave propagation in laterally heterogeneous anelastic media: theory and applications to seismic zonation, Adv. Geophys., *43*, 1–95.

Panza, G. F., Irikura, K., Kouteva, M., Peresan, A., Wang, Z., and R. Paragoni (2011), Advanced seismic hazard assessment, Pure App. Geophys., *169*, 1–9, doi:10.1007/s00024-010-0179-9.

Panza, G. F., La Mura, C., Peresan, A., Romanelli, F., and F. Vaccai (2012), Seismic hazard scenarios as preventive tools for a disaster resilient society, Advances in Geophysics, *53*, 93–165.

Press, W. H., Teukolsky, B. P., and W. T. Vetterling (1992), *Numerical Recipes*, 2nd ed., Cambridge University Press, New York.

Putelat, T., Dawes, J. H. P., and J. R. Willis (2008), On the seismic cycle seen as a relaxation oscillation, Phil. Mag., *88*, Nos. 28–29, 3219–3243, doi:10.1080/14786430802216374.

Putelat, T., Dawes, J. H. P., and J. R. Willis (2010), Regimes of frictional sliding of a spring–block system, J. Mech. Phys. Solids, *58*, 27–53.

Putelat, T., Willis, J. R., and J. H. P. Dawes, (2012), Wave-modulated orbits in rate-and-state-friction, Int. J. Non-Lin. Mech., *47*, 258–267, doi:10.1016/j.ijnonlinmec.2011.05.016.

Ranjith, K., and J. R. Rice (1999), Stability of quasi–static slip in a single degree of freedom elastic system with rate and state dependent friction, J. Mech. Phys. Sol., *47*, No. 6, 1207–1218.

Rice, J. R. (1993), Spatio-temporal complexity of slip on a fault, J. Geophys. Res., *98*, No. B6, 9885–9907.

Reid, H. F. (1910), The California earthquake of April 18, 1906. Report of the State Investigation Commission, The Mechanics of the Earthquake, vol. 2. Carnegie Inst., Washington, DC.

Ripperger, J., Mai, P. M., and J.-P. Ampuero (2008), Variability of near–field ground motion from dynamic earthquake rupture simulations, Bull. Seismol. Soc. Am., *98*, 1207–1228.

Ruina, A. L. (1983), Slip instability and state variable friction laws, J. Geophys. Res., *88*, 10,359–10,370.

Rice, J. R. and S. T Tse (1986), Dynamic motion of a single degree of freedom system following a rate and state dependent friction law, J. Geophys. Res., *91*, 521–530.

Scholz, C. H., and J. T. Engelder (1976), The role of asperity indentation and ploughing in rock friction: I. Asperity creep and stick–slip, Int. J. Rock Mech. Min. Sci. Geomech. Abstr., *13*, 149–154.

Song, S. G., and P. Somerville (2010), Physics–based earthquake source characterization and modeling with geostatistics, Bull. Seismol. Soc. Am., *100*, No. 2, 482–496.

Thompson, J. M. T., and H. B. Stewart (2002), *Nonlinear Dynamics and Chaos*, 2nd ed., John Whiley and Sons, New York.

Tinti, E., Bizzarri, A., and M. Cocco (2005), Modeling the dynamic rupture propagation on heterogeneous faults with rate– and state–dependent friction, Ann. Geophys., *48*, No. 2, 327–345.

Vere-Jones, D. (2010), Foundations of statistical seismology, Pure Appl. Geophys., *167*, 645–653, doi:10.1007/s00024-010-0079-z.

Weatherley, D., and S. Abe (2004), Earthquake statistics in a block slider model and a dully dynamic fault model, Nonlin. Proc. Geophys., *11*, 553–560.

Weeks, J. D. (1993), Constitutive laws for high–velocity frictional sliding and their influence on stress drop during unstable slip, J. Geophys. Res., *98*, No. B10, 17,637–17,648.

Wyss, M., Nekrasova, A. K., and V. G. Kossobokov (2012), Errors in expected human losses due to incorrect seismic hazard estimates, Natural Hazards, doi:10.1007/s11069-012-0125-5.

Xu, H.-J. and L. Knopoff (1994), Periodicity and chaos in a one-dimensional model of earthquakes, Phys. Rev. E, *50*, 5, 3577–3581.

Zuccolo, E., Vacari, F., Peresan, A., and G. F. Panza (2011), Neo-deterministic and probabilistic hazard assessments: a comparison over the Italian territory, Pure Appl. Geophys., *168*, 69–83, doi:10.1007/s.00024-010-0151-8.

(Received March 18, 2013, revised November 11, 2013, accepted November 14, 2013, Published online December 14, 2013)